HTD-Vol. 335, Proceedings of the ASME Heat Transfer Division
Volume 4
ASME 1996

MEASUREMENTS AND MODELING OF SOOT FORMATION AND RADIATION IN MICROGRAVITY JET DIFFUSION FLAMES

Jerry C. Ku*
Mechanical Engineering Department
Wayne State University

Li Tong#
Mechanical Engineering Department
Wayne State University

Paul S. Greenberg
Microgravity Combustion Branch
NASA Lewis Research Center

ABSTRACT

This is a computational and experimental study for soot formation and radiative heat transfer in jet diffusion flames under normal gravity (1-g) and microgravity (0-g) conditions. Instantaneous soot volume fraction maps are measured using a full-field imaging absorption technique developed by the authors. A compact, self-contained drop rig is used for microgravity experiments in the 2.2-second drop tower facility at NASA Lewis Research Center. On modeling, we have coupled flame structure and soot formation models with detailed radiation transfer calculations. Favre-averaged boundary layer equations with a k-ε-g turbulence model are used to predict the flow field, and a conserved scalar approach with an assumed β-pdf are used to predict gaseous species mole fraction. Scalar transport equations are used to describe soot volume fraction and number density distributions, with formation and oxidation terms modeled by one-step rate equations and thermophoretic effects included. An energy equation is included to couple flame structure and radiation analyses through iterations, neglecting turbulence-radiation interactions. The YIX solution for a finite cylindrical enclosure is used for radiative heat transfer calculations. The spectral absorption coefficient for soot aggregates is calculated from the Rayleigh solution using complex refractive index data from a Drude-Lorentz model. The exponential-wide-band model is used to calculate the spectral absorption coefficient for H_2O and CO_2. It is shown that, when compared to results from true spectral integration, the Rosseland mean absorption coefficient can provide reasonably accurate predictions for the type of flames studied. The soot formation model proposed by Moss, Syed, and Stewart seems to produce better fits to experimental data and more physically sound than the simpler model by Khan et al. Predicted soot volume fraction and temperature results agree well with published data for a normal gravity co-flow laminar flames and turbulent jet flames. Predicted soot volume fraction results also agree with our data for 1-g and 0-g laminar jet flames as well as 1-g turbulent jet flames.

* Corresponding author.
# Presently Design Engineer, Caterpillar Co., Aurora, IL 60507.

NOMENCLATURE

b	constant in the model for modified equilibrium temperature
$C_{(\,)}$	rate constant for nucleation (α,δ), growth (β), coagulation (γ), or oxidation (χ)
C_k	rate constant in the model by Khan et al., Eq. (9), $C_k = 16.8$ kg/Nms
E_s	activation energy in the model by Khan et al., Eq. (9), E_s = 40000 cal/mole
f	gas mixture fraction
f_v, $\hat{f}_v$	soot particle volume fraction, and $\hat{f}_v = \rho_s f_v/\rho$
g	variance of f
H	total enthalpy
k	turbulent kinetic energy
ℓ	a length scale in the heat sink model
$m_{(\,)}$	exponent on the mole fraction in rate equations for nucleation (α) or coagulation (γ)
N, $\hat{N}$	soot particle number density, and $\hat{N} = N/(\rho n_0)$
n_0	Avogadro's number, $n_0 = 6\times10^{26}$
P_{fu}	partial pressure of unburned fuel
q_r, $\vec{q}_r$	radiative heat flux and radiative heat flux vector, respectively
r	radial distance from the flame axis
S_ϕ	source term for property ϕ in Eq. (1)
T	flame temperature
T_{eq}	equilibrium (adiabatic) flame temperature
$T_{eq,max}$	maximum equilibrium (adiabatic) flame temperature
T_∞	surroundings temperature
$T_{(\,)}$	activation temperature in rate equations for nucleation (α), coagulation (γ), or oxidation (χ)
u, v	axial and radial gas velocity component, respectively
v_t	radial direction thermophoretic velocity for soot particles
x	axial distance from the nozzle exit
X	gas species mole fraction
α	soot particle nucleation rate, in the particle transport equation for number density
β	soot particle surface growth rate

γ soot particle coagulation rate

δ soot particle nucleation rate, in the particle transport equation for volume fraction

ε emissivity of soot/gas mixture

e turbulent dissipation energy

χ soot particle oxidation rate

$\mu_{eff,\phi}$ effective viscosity in Eq. (1)

ρ mass density of gas mixture

ρ_s mass density of soot particles

σ Stefan-Boltzmann constant, $\sigma = 5.670 \times 10^{-8}\ \mathrm{W/m^2K^4}$

ϕ a general variable representing 1, $\bar{u}$, $\bar{f}$, k, e, g, $\hat{f}_v$, $\hat{N}$, or H

φ local fuel/air equivalence ratio

INTRODUCTION

The subject of soot formation and radiation heat transfer in microgravity jet diffusion flames is important not only for the understanding of fundamental transport processes involved but also for providing findings relevant to spacecraft fire safety and soot emissions and radiant heat loads of combustors used in air-breathing propulsion systems. The longer flame residence time and the dominance of effects such as thermophoresis and diffusion, both as a result of eliminating buoyancy-induced convective flow, make microgravity an ideal environment for studying diffusion flame fundamentals. Comparisons between normal gravity (1-g) and microgravity (0-g) results, and between measurements and model predictions, will be used to improve our understanding about diffusion flames. Considerable amount of data have been published on microgravity jet diffusion flames (Bahadori and Edelman, 1993). Most of these data are from photographic measurements, with some wide-angle radiometry, far-field temperature and gas species measurements. Our objective is to provide local measurements and modeling for soot volume fraction, flame temperature, and radiative heat fluxes in microgravity jet diffusion flames.

In terms of our fundamental understandings of normal gravity diffusion flames, it is believed that gas-phase processes in laminar and turbulent flames are similar and relatively well known, with turbulent flames usually approximated as wrinkled laminar flames, known as the laminar flamelet concept (Bilger, 1976, 1977; Faeth and Samuelson, 1986; Sivathanu and Faeth, 1990b). However, this similarity becomes somewhat conditional or invalid for soot and radiation properties (Gore and Faeth, 1986; Sivathanu and Faeth, 1990a; Sivathanu et al., 1990). Both soot formation and radiation heat transfer are inherently difficult subjects. Soot inception is much slower than gas-phase reactions, soot particles have much smaller diffusivities, and their growth, coagulation, and oxidation have not been well understood. The difficulties in treating detailed radiation heat transfer are to find accurate, yet computationally efficient, solutions for nonhomogeneous and nongray media, as well as accurate models for soot and gas radiative properties and for turbulence-radiation interactions.

Our approach is to use simple, yet established, models for flame structure, which include Favre-averaged boundary-layer-type governing equations with a k-e-g turbulence model for flow field and a conserved scalar approach with an assumed β-pdf (probability density function) for gaseous species concentration profiles. Soot transport is described as that of a scalar property, including thermophoretic effects. Two existing soot formation models, with some improvements, will be tested and compared. Both models use one-step reactions to describe various mechanisms in soot formation. Radiative heat flux and its divergence are calculated using the YIX solution (Tan et al., 1990; Hsu et al., 1993), which is a numerical solution for the integral formulation of the radiative transfer equation. Total radiative properties, such as the Rosseland and the Planck means, are introduced to reduce computational times. Results based on these means are compared against results from detailed spectral integration. The flame structure solver and the radiation heat transfer solver are coupled through an energy equation, and they are solved iteratively until a set convergence is achieved.

Predicted soot volume fraction and flame temperature results are compared to published data for 1-g co-flow laminar flames, as well as for 1-g and 0-g jet laminar and turbulent flames.

MODELING OF JET DIFFUSION FLAME STRUCTURE

The structure of turbulent jet diffusion flames is modeled using the Favre-averaged equations for conservation of mass, momentum, and mixture fraction. A conserved scalar approach (Bilger, 1976; Jeng and Faeth, 1984; Gore and Faeth, 1984) with an assumed probability density function (pdf) and a k-e-g turbulence model (Lockwood and Naguib, 1975) are used. All governing equations can be written in a general form as (Faeth et al., 1985)

$$\frac{\partial}{\partial x}(\bar{\rho}\bar{u}\phi) + \frac{1}{r}\frac{\partial}{\partial r}(r\bar{\rho}\bar{v}\phi) = \frac{1}{r}\frac{\partial}{\partial r}\left(r\mu_{eff,\phi}\frac{\partial \phi}{\partial r}\right) + S_\phi \ , \qquad (1)$$

where ϕ = 1, $\bar{u}$ (velocity), $\bar{f}$ (mixture fraction), k (kinetic energy), e (dissipation), or g (variance of f). Details for $\mu_{eff,\phi}$ (effective viscosity), S_ϕ (source) and assumptions are given in those references. Buoyancy effect is considered in mean flow only, neglecting buoyancy-turbulence interactions. For laminar flames, Eq. (1) is simplified accordingly.

The system represented by Eq. (1) is solved using the block-tridiagonal code of Chen et al. (1987). State relationships constructed from equilibrium calculations using STANJAN (Reynolds, 1986) are introduced to decouple chemical reactions from flow calculations. More accurate laminar flamelet approaches (Bilger, 1977; Rogg, 1993) will be considered in the future.

MODELING OF SOOT FORMATION AND OXIDATION

We have considered two sets of soot formation and oxidation models. Both describe the transport of soot particles as that of a scalar property using Eq. (1). For soot transport in laminar flames, a radial thermophoretic velocity term, $v_t = -.054(\nu/T)(\partial T/\partial r)$, is added. The two-equation model (Moss et al., 1988; Syed et al.,1990) is based on number density (N) and volume fraction (f_v), and the two respective source terms are

$$S_{\hat{N}} = \bar{\alpha} - \bar{\beta}\bar{\rho}^2\hat{N}^2 - n_0^{1/3}\bar{\chi}\bar{\rho}\hat{f}_v^{-1/3}\hat{N}^{4/3} \ , \quad \phi = \hat{N} \equiv \frac{N}{\rho n_0} \ ; \qquad (2)$$

$$S_{\hat{f}_v} = n_0^{1/3}(\bar{\gamma} - \bar{\chi})\bar{\rho}\hat{f}_v^{2/3}\hat{N}^{1/3} + \bar{\delta} \ , \quad \phi = \hat{f}_v \equiv \frac{\rho_s f_v}{\rho} \ ; \qquad (3)$$

where $n_0 = 6 \times 10^{26}$ is Avogadro's number and ρ_s = 1.8 g/cm^3 is mass density of soot. Soot oxidation models of Leung et al. (1991) and

Fairweather et al. (1992) are modified to include oxidation by both O_2 and OH. Rate-equations of Arrhenius type are used to model nucleation (α), growth (β), coagulation (γ) and oxidation (χ). These rate equations are given as

$$\alpha = C_\alpha \rho^2 X_C^{m_\alpha} \sqrt{T} \exp(-T_\alpha / T), \tag{4}$$

$$\beta = C_\beta \sqrt{T}, \tag{5}$$

$$\gamma = C_\gamma \rho X_C^{m_\gamma} \sqrt{T} \exp(-T_\gamma / T), \tag{6}$$

$$\delta = C_\delta \alpha, \tag{7}$$

$$\chi = C_\chi (X_{OH} + X_{O_2}) \sqrt{T} \exp(-T_\chi / T), \tag{8}$$

where T is flame temperature, T_α, T_γ, T_χ are activation temperatures, ρ is mixture density, X_C is fuel mole fraction, and X_{OH} and X_{O_2} are mole fractions for OH and O_2, respectively. Numerically, any combinations of rate constants (C_α, C_β, C_γ, C_δ, C_χ), activation temperatures (T_α, T_γ, T_χ), and exponents (m_α, m_γ) can be adjusted to produce a optimal fit between model predictions and experimental data.

Another model is a one-equation model, based on volume fraction only, developed by Khan et al. (1971; 1974). This model characterizes soot formation by an Arrhenius-type equation, and the corresponding source term is

$$S_{\hat{f}_v} = C_k P_{fu} \varphi^{m_k} \left(\frac{\rho}{\rho_s} \right) \exp\left(-\frac{E_s}{RT} \right), \quad \phi = \hat{f}_v \equiv \frac{\rho_s f_v}{\rho}; \tag{9}$$

where C_k is the rate constant, P_{fu} denotes the partial pressure of unburned fuel, φ is the local fuel/air equivalence ratio, and E_s is the activation energy. The soot oxidation model of Lee et al. (1962) is adopted, which is similar to Eq. (9), with $\varphi^{m_k}(\rho/\rho_s)$ replaced by $\hat{f}_v / \sqrt{T}$. Although the model by Khan et al. is simpler, it seems less physically sound than that by Moss et al., since it does not include such mechanisms as coagulation which causes decreasing number density under constant volume fraction.

SOLUTION FOR FLAME RADIATION HEAT TRANSFER

Although it plays an important role, radiation transfer has been neglected in detailed combustion analyses due to such difficulties as the computational demands and accuracy of various solution methods (Tong and Skocypec, 1992), the coupling of radiation and flame structure solvers, the accuracy of spectral radiative properties, and efficient methods for integrating fluxes and other quantities over the spectral range.

We chose the recently developed YIX method (Tan et al., 1990; Hsu et al., 1993) for calculating the radiative heat flux $\vec{q}_r$ and its divergence. A solution derived by Hsu and Ku (1994) for finite axisymmetric cylindrical enclosures is used for radiation calculations from diffusion flames. The YIX method is a numerical approach for solving the integral formulation of the radiative transfer equation by reducing the order of the multiple distance-angular integrals. The name YIX comes from the shape of the pattern of integration points for three, two, and four angular directions. One important attribute of this method is that these integration points can be pre-calculated and stored, significantly reducing computational time. For multi-dimensional geometries, discrete ordinate sets are used for angular quadratures. Although computationally quite intensive, the YIX method has proven to be very accurate and suitable for nonhomogeneous media (Hsu and Ku, 1994; Hsu and Ku 1995). Simplified models such as a fixed percentage of local heat loss from equilibrium everywhere, a temperature modified from that under equilibrium as $T = T_{eq}[1 - b(T_{eq}/T_{eq,max})^4]$ (Leung et al., 1991), or a heat sink term given as $S_\phi = -\varepsilon\sigma(T^4 - T_-^4)/\ell$ (Kent and Honnery, 1987) has each been tested and found inaccurate. We also derived a spherical harmonics (P_N) approximate solution for nonhomogeneous media following the work of Menguc and Viskanta (1986), but found the resulting partial differential equations numerically unstable for enclosures involving optically thin regions such as in diffusion flames.

The radiation solver is coupled to the flame structure solver through the energy equation. For diffusion flames, the energy equation takes the same form as Eq. (1), with $\phi = H$ (total enthalpy) and $S_\phi = -\nabla \cdot \vec{q}_r$, and the latter is calculated from a solution for the radiative transfer equation. These two solvers, both depending on the temperature, are numerically incompatible. The solver for flame structure, soot transport, and the energy equation solves parabolic differential equations of Eq. (1) type. The solver for radiative transfer, YIX or otherwise, is inherently not parabolic, since radiation is an integral phenomenon over all distances and solid angles. We chose an iterative approach and used temperature as the convergence criterion. The iteration starts with the flame structure solver using an initial guess based on $S_\phi = -\varepsilon\sigma(T^4 - T_-^4)/\ell$ to calculate velocities, gas and soot concentrations, density, and flame temperature. The resulting temperature is used for calculating $\nabla \cdot \vec{q}_r$ from the YIX solver. The resulting $\nabla \cdot \vec{q}_r$ is substituted back into the structure solver to update (by averaging the two latest runs) velocities, concentrations, density, and temperature. This process is repeated until a convergence on the temperature is accomplished between two subsequent iterations ($\Delta T / T < 0.002$). Figure 1 shows a flow chart for the computational procedure. For flames calculated here, it typically takes less than 10 iterations to reach the convergence (Tong, 1995; Ku et al., 1995b). The turbulence-radiation interactions, which are shown to be significant by Gore et al. (1992), will be included in the future.

To evaluate spectral radiative properties, the absorption coefficient for soot aggregate is calculated from the Rayleigh solution (Ku and Shim, 1991) using the refractive index calculated from Habib and Vervisch's (1988) Drude-Lorentz dispersion model. Scattering from soot particles is neglected at present to reduce computational time, but will be included in the future. The exponential-wide-band model of Edwards (1976) is used to calculate the absorption coefficient for CO_2 and H_2O gases. The most accurate way to evaluate the total (i.e., over the spectral range) fluxes and flux divergence is to first calculate them for each spectral increment and then calculate the integrals. This is computationally inefficient because of the iterations required between the flame structure and radiation solver. To focus on the iterations, we choose to test the Planck (a_P) and the Rosseland (a_R) mean absorption coefficients given as (Siegel and Howell, 1992)

$$a_P(T,P) = \frac{1}{\sigma T^4} \int_0^\infty a_\lambda(\lambda,T,P) e_{\lambda b}(\lambda,T)\, d\lambda,$$

$$a_R(T,P) = \left[\int_0^\infty \frac{1}{a_\lambda(\lambda,T,P)} \frac{\partial e_{\lambda b}(\lambda,T)}{\partial e_b(T)}\, d\lambda \right]^{-1}. \tag{10}$$

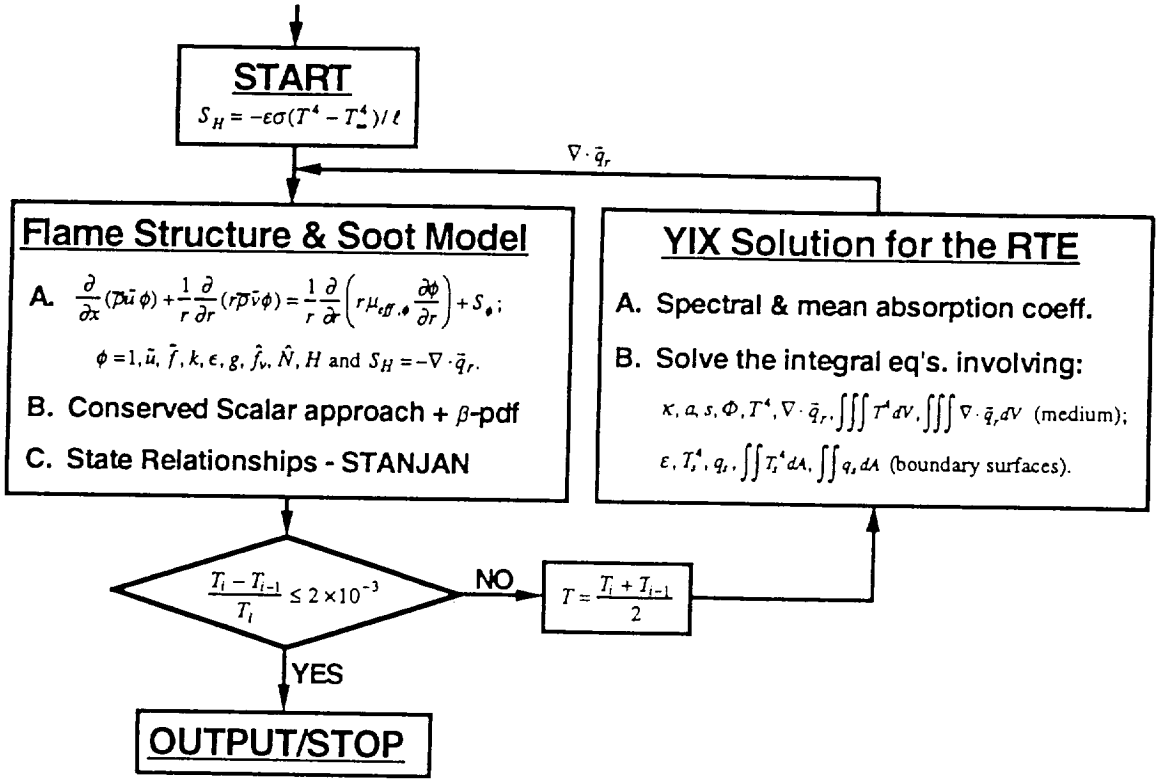

Figure 1. A flow chart for computational procedures of solving flame structure and radiation through iteration.

RESULTS AND DISCUSSION

We first compared the radiation heat transfer results from a true spectral integration (1 to 20 μm) against those from mean coefficients using pre-calculated temperature and particle and gas concentrations distributions for a turbulent ethylene diffusion flame. Figure 2 shows a comparison of the soot/gas mixture spectral absorption coefficient at a specified condition against both means. Figure 3 shows that the flux divergence based on the Rosseland mean and on integration agree quite well. We thus base all subsequent calculations on the Rosseland mean coefficient. However, it should be noted that the accuracy of radiative property values, especially those for soot, requires further study.

We next tried to identify whether the soot formation model by Moss et al. or that by Khan et al. is more accurate by fitting predicted flame temperature and soot volume fraction against experimental data for a 3.85 cc/s co-flow laminar ethylene flame (Santoro et al.; 1983, 1987). The results are shown in Figure 4. The agreements are reasonably good, indicating that the models seem to be physically sound. Values for rate constants in Moss' model are listed in Table 1. For Khan's model, we used C_k = 16.8 kg/Nms, m_k = 3, and E_s = 40000 cal/mole. Although both models yield similar fit to experimental data, other calculations reveal that Khan's model is overly sensitive to temperature and tend to over-predict centerline volume fraction distributions. We therefore chose Moss' model for all subsequent calculations. Figure 4(a) also shows that the inclusion of radiative transfer does provide a more accurate magnitude and trend in temperature profiles than adiabatic values. Figure 4(c) shows that the temperature converges smoothly in less than 10 iterations. Both models yield fairly accurate predictions for gas velocity (Tong, 1995). It should be pointed out that, except for the work by Fairweather et al. (1992), other works on soot modeling (Moss et al., 1988; Syed et al., 1990; Kennedy et al., 1990; Kennedy et al., 1991) made comparisons against soot volume fraction data only. We base our comparisons on all available gas velocity, temperature, and soot volume fraction data.

We then examined the generality of Moss' model by fitting predictions to experimental data. We used two groups of data, one from Santoro et al., (1983, 1987) with the same fuel and burner but at different flow rates, and the other from Greenberg and Ku (1996b) for 1-g and 0-g 2.30 cc/s laminar jet acetylene flames. Table 1 lists burner dimensions and flow conditions for these flames. Table 2 lists values of rate constants which produce a reasonable fit for soot volume fraction between model predictions and data, as shown in Figures. 5 through 10. We adjusted all rate constants (C_α, C_β, C_γ, C_δ, C_χ) to find a reasonable fit. Even though activation temperatures (T_α, T_γ, T_χ) and exponents (m_α, m_γ) can also be adjusted for possibly better fits, we chose to use the same values as those in the original works, since our experience indicates that these parameters are less influential (Tong, 1995).

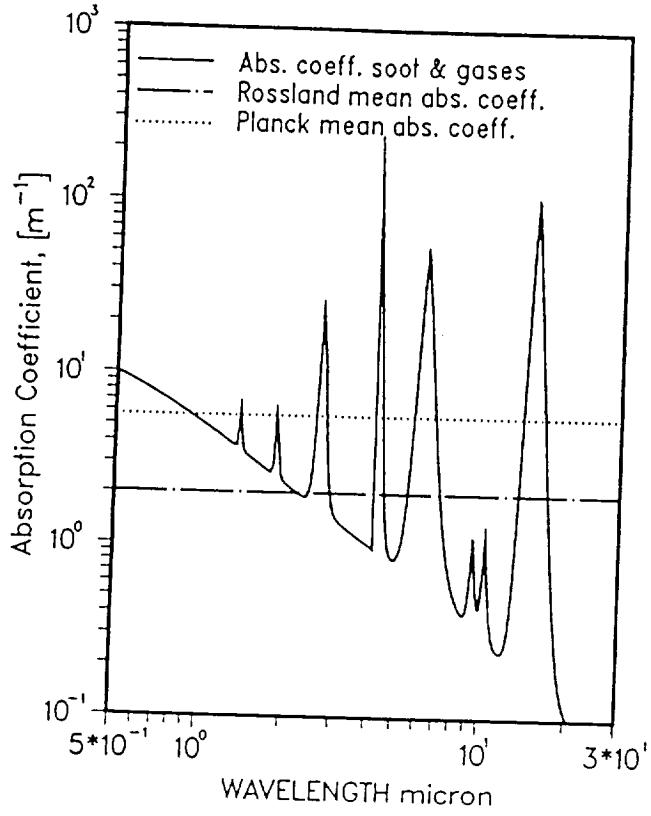

Figure 2. Absorption coefficients for soot/gases mixture at 1400K, with 0.1 mole fraction for CO_2 and H_2O, and a soot volume fraction of 10^{-6}.

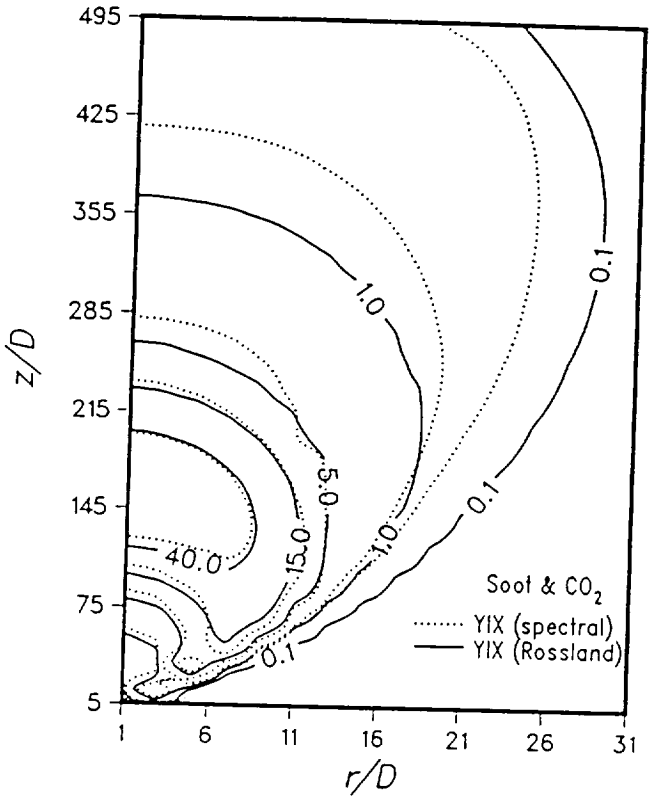

Figure 3. The flux divergence contours for a simulated ethylene jet flame (D = 0.58 mm, $\dot{Q}$ = 3.96 cm³/sec, and Re = 536).

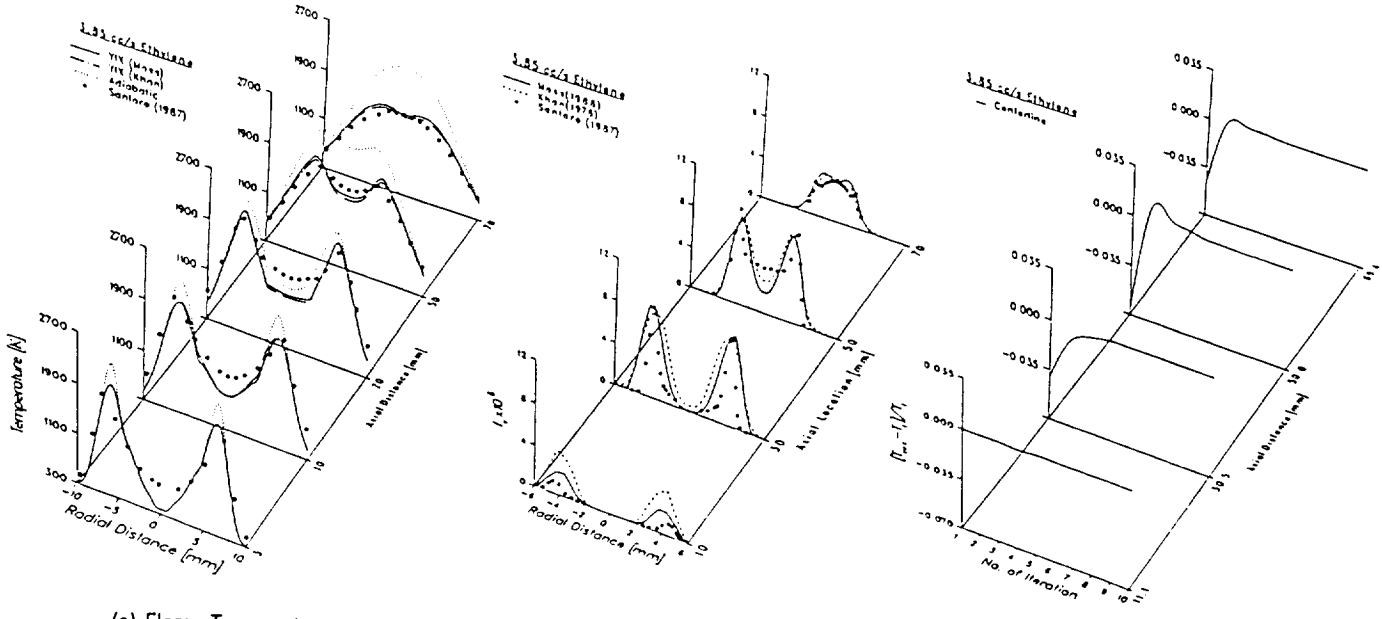

(a) Flame Temperature (b) Soot Volume Fraction (c) Convergence of Temperature

Figure 4. Comparisons of predictions to data, and the convergence on temperature over iterations, for a 3.85 cc/s laminar ethylene co-flow flame.

Table 1 Burner Dimension and Flow Conditions for Flames in This Study

Fuel	D_{fuel} (mm)	D_{air} (mm)	Q_{fuel} (cc/s)	V_{fuel} (cm/s)	$Re_{D_{fuel}}$	Q_{air} (cc/s)	V_{air} (cm/s)
Ethylene (C_2H_4)	11.1	101.6	2.30	2.38	16.3	713.3	8.90
Ethylene (C_2H_4)	11.1	101.6	3.85	3.98	27.2	713.3	8.90
Ethylene (C_2H_4)	11.1	101.6	4.90	5.06	34.7	1068.3	13.3
Acetylene (C_2H_2)	1.65	NA	2.30	107.7	179.4	NA	NA
Ethylene (C_2H_4)	3.0	NA	36757	5200	11725	NA	NA
Acetylene (C_2H_2)	0.508	NA	10.0	4933.8	2550	NA	NA

Table 2 Values of Soot Formation Rate Constants for Flames in This Study

Flames	$C_\alpha \times 10^{-7}$	$C_\beta \times 10^{-4}$	$C_\gamma \times 10^{16}$	C_δ	$C_\chi \times 10^{-2}$
2.30 cc/s C_2H_4 (1-g)	0.7	1.0	0.62	144	1.4
3.85 cc/s C_2H_4 (1-g)	2.0	1.0	0.62	144	1.4
4.90 cc/s C_2H_4 (1-g)	3.0	1.0	0.62	144	1.4
2.30 cc/s C_2H_2 (1-g)	5.8	1.0	0.62	144	3.62
2.30 cc/s C_2H_2 (0-g)	2.7	1.0	0.62	144	2.17
2.30 cc/s C_2H_2 (1-g) $[m_\alpha = m_\gamma = 4]$	320.0	1.0	39.7	144	2.41
2.30 cc/s C_2H_2 (0-g) $[m_\alpha = m_\gamma = 4]$	230.4	1.0	39.7	144	2.16
0.61 lpm C_2H_4 (1-g)	0.2275	1.3×10^3	2.0×10^{13}	5040	0.002
10.0 cc/s C_2H_2 (1-g)	0.2275	1.3×10^3	2.0×10^{13}	5040	0.002

Note: SI units. In all cases, $T_\alpha = 46100$ K, $T_\gamma = 12600$ K, and $T_\chi = 19680$ K. Unless specified otherwise, $m_\alpha = m_\gamma = 1$.

Numerically, we feel the fits can be improved, but we would like to examine the aspect of improving the models themselves first. As can be seen from the figures, the 4.90 cc/s ethylene and both 1-g and 0-g 2.30 cc/s acetylene flames are smoking (i. e., releasing soot particles from the flame tip), while others are non-smoking. In Figures 5 and 6, for 4.90 and 2.30 cc/s respectively, we included a dashed curve for predictions using the same rate constants as those for 3.85 cc/s. This shows that Moss' model is not sensitive enough to changes in fuel flow rate. However, this can be easily improved by adjusting C_α, the nucleation rate constant. The fact that the fit looks better for 2.30 cc/s flame (Figure 6) than for 4.90 cc/s flame (Figure 5) suggests that further adjustments of rate constants may be required going from non-smoking (2.30 and 3.85 cc/s) to smoking flames (4.90 cc/s).

When applied the models to 1-g and 0-g laminar jet acetylene flames, we first tried to fit the data by adjusting the rate constants C_α and C_χ only, while keeping $m_\alpha = m_\gamma = 1$. The results are shown in Figures 7 and 8. The fits are obviously not as good as those for co-flow ethylene flames, and perhaps expectedly so due to the fundamental differences between jet flames and co-flow flames. However, further adjustments on model coefficients, including setting $m_\alpha = m_\gamma = 4$, yield better fits, as shown in Figures 9 and 10. Notice that the fits to 1-g and 0-g flame are obtained with only minor adjustments to C_α and C_χ.

Based on the facts that the model can produce reasonably accurate fits to data for flames of different types, flow rates, fuels, and 1-g/0-g conditions, we feel that Moss' model is physically sound. Some patterns about the effects of each model coefficient on the soot volume fraction distribution are identified as follows.

1. The overall shape and peak locations of volume fraction distribution are fairly independent of all rate constants (C_α, C_β, C_γ, C_δ, C_χ).
2. An increase in nucleation (C_α) or surface growth (C_γ) rate constant will cause an overall increase in soot volume fraction, with higher sensitivity to C_γ than to C_α.
3. Coagulation (C_β) and oxidation (C_χ) rate constants have negligible effects on volume fraction distributions near the burner exit, but have significant effects at higher locations in the flame. An increase in C_χ will cause a decrease around the edge, and an increase in C_β will cause a decrease around the center region of the flame.
4. An increase in both exponents (m_α, m_γ) will cause an increase in soot volume fraction around the centerline region at higher locations in the flame, and will shift the soot volume fraction peak locations inward (toward fuel-rich side, as if the soot yield were dependent on an intermediate species rather than the parent fuel).
5. An increase in thermophoretic velocity v_t will cause an increase in soot volume fraction around the centerline region.

Finally, we tested the model on turbulent jet flames. We compared against the published data of Kent and Honnery (1987) for a 1-g ethylene flame, and against our data for a 1-g acetylene flame. Figure 11 shows comparisons of two model predictions, one using the YIX solver and the other using the simple sink term, against Kent and Honnery's (1987) data. Figure 12 shows predicted volume fraction maps for 1-g and 0-g acetylene flames, and a comparison against our 1-g data. Again, the model was able to predict the correct level and overall shape of volume fraction and temperature distributions, even though we only made limited adjustments and used the same rate coefficients for both flames, due to the excessive computational time required and modeling uncertainties in turbulence-radiation interactions and radiative properties. In Figure 11, the discrepancy may be caused by the missing turbulence-radiation effects. In Figure 12, we can modify the oxidation constant (C_χ) to get a better fit. The burner dimension and flow conditions and rate coefficients for these flames are listed in Tables 1 and 2. The noticeable differences in rate coefficients between turbulent and laminar flames are consistent with Moss' published values.

We plan to adopt more accurate means of evaluating total radiative quantities, such as the wide-band model used by Song and Viskanta (1987). Their derivation of a "mean" radiative transfer equation to include turbulence-radiation effects is also worth noting. A joint pdf (Gore et al., 1992; Janika and Kollmann, 1987)) could be developed to correlate enthalpy, temperature, and mixture fraction for modeling turbulence-radiation effects,. Turbulence-buoyancy interactions (e. g., Fairweather et al., 1992) will be examined for 0-g flames.

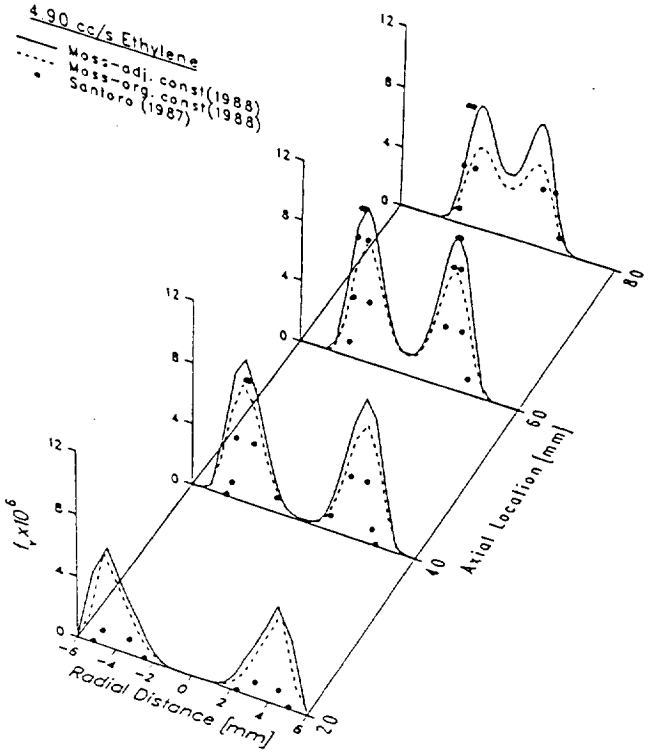

Figure 5. Comparisons of predictions to data for a 4.90 cc/s laminar ethylene co-flow flame. Dashed curves are based on rate constants for 3.85 cc/s flame.

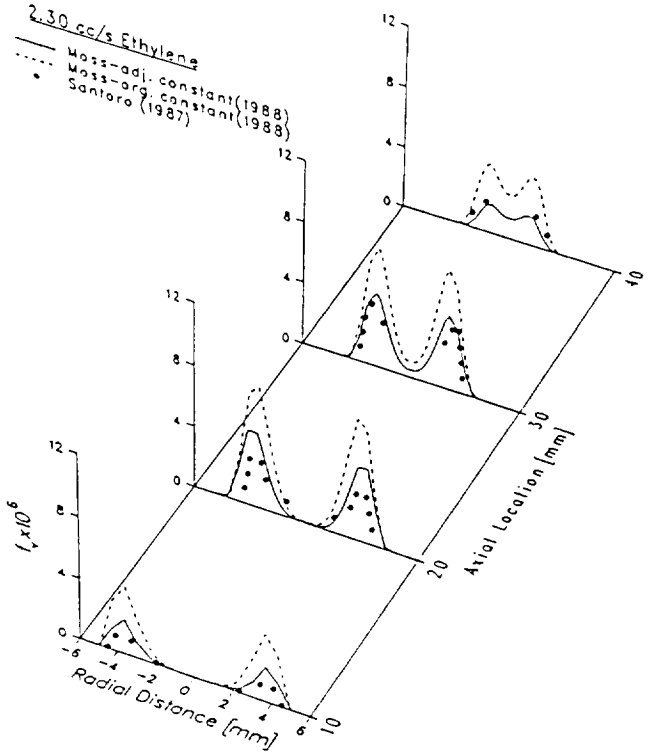

Figure 6. Comparisons of predictions to data for a 2.30 cc/s laminar ethylene co-flow flame. Dashed curves are based on rate constants for 3.85 cc/s flame.

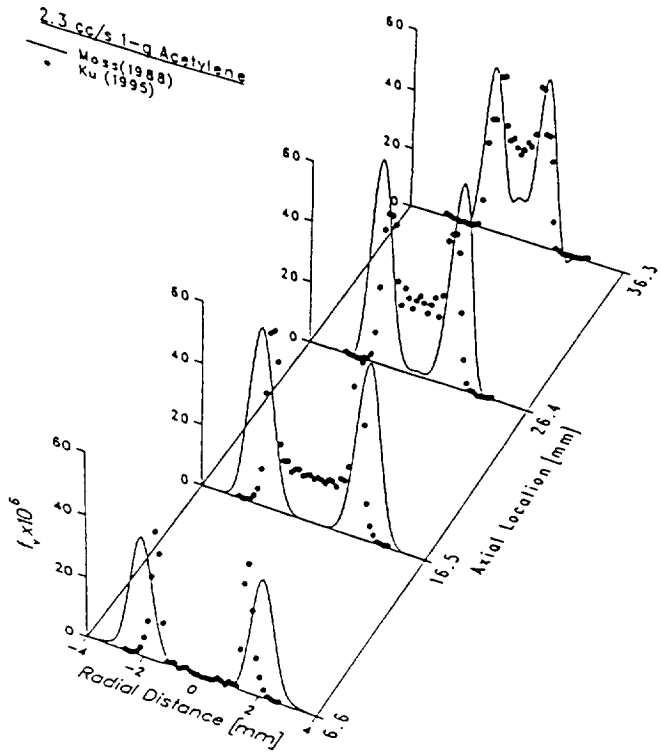

Figure 7. Comparisons of predictions to data for a 1-g 2.30 cc/s laminar acetylene jet flame. [$m_\alpha = m_\gamma = 1$]

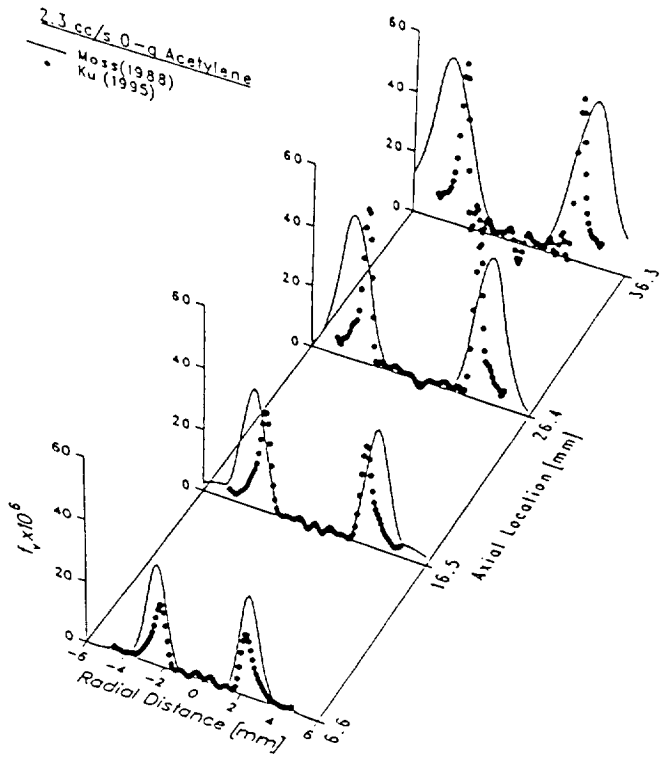

Figure 8. Comparisons of predictions to data for a 0-g 2.30 cc/s laminar acetylene jet flame. [$m_\alpha = m_\gamma = 1$]

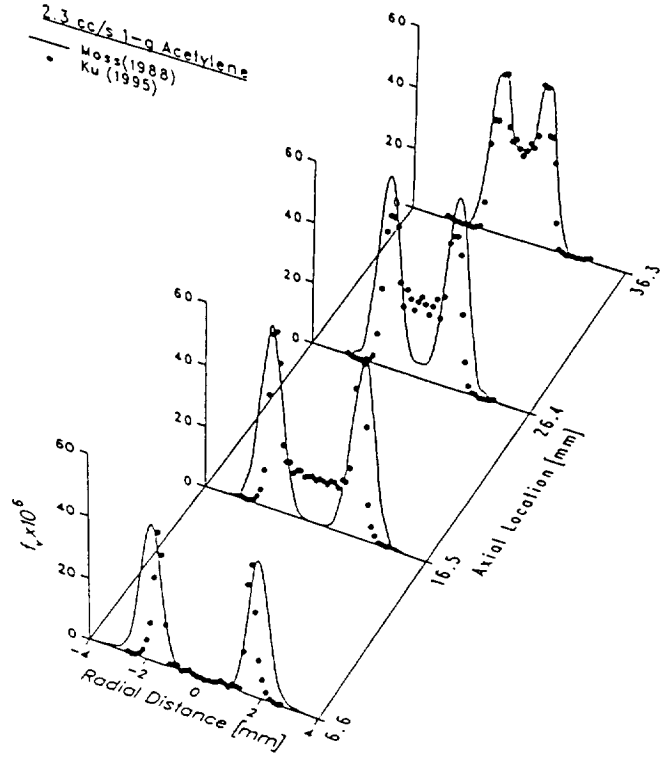

Figure 9. Comparisons of predictions to data for a 1-g 2.30 cc/s laminar acetylene jet flame. [$m_\alpha = m_\gamma = 4$]

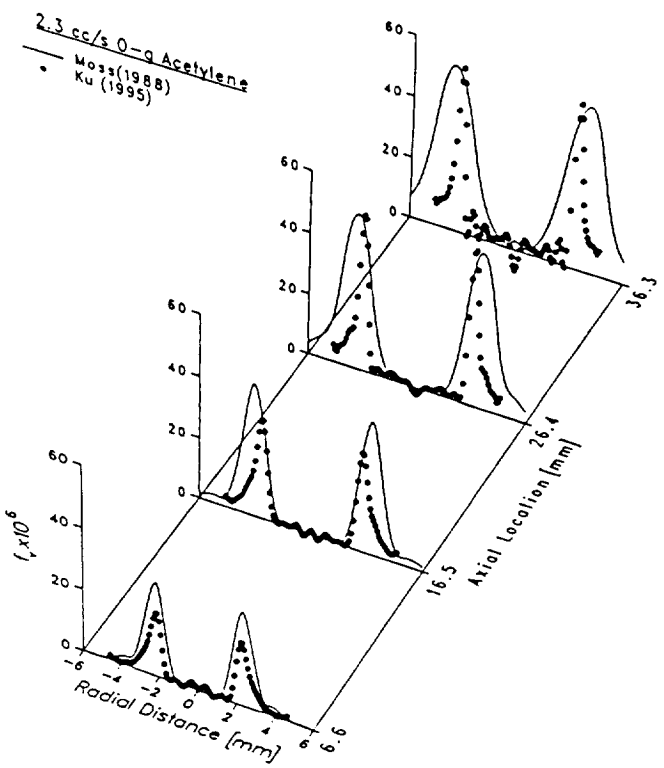

Figure 10. Comparisons of predictions to data for a 0-g 2.30 cc/s laminar acetylene jet flame. [$m_\alpha = m_\gamma = 4$]

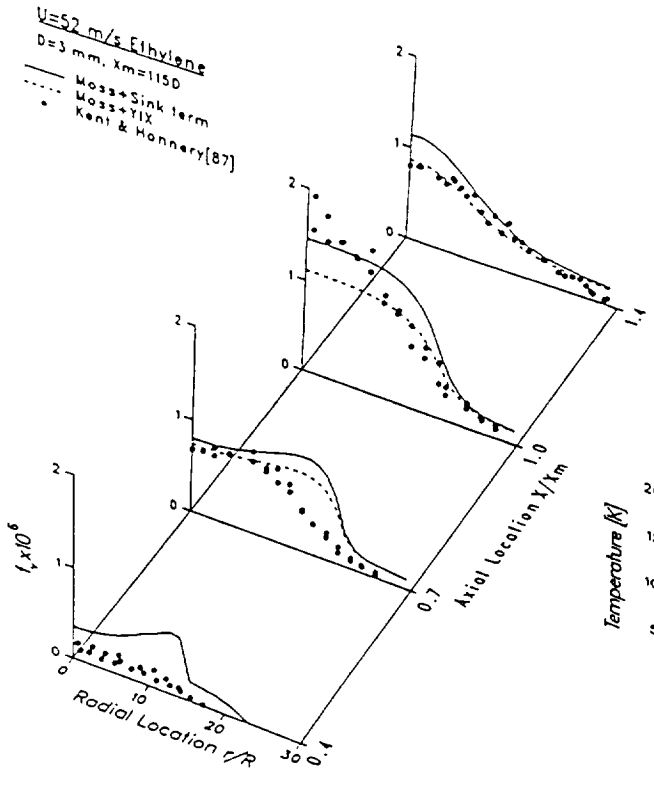

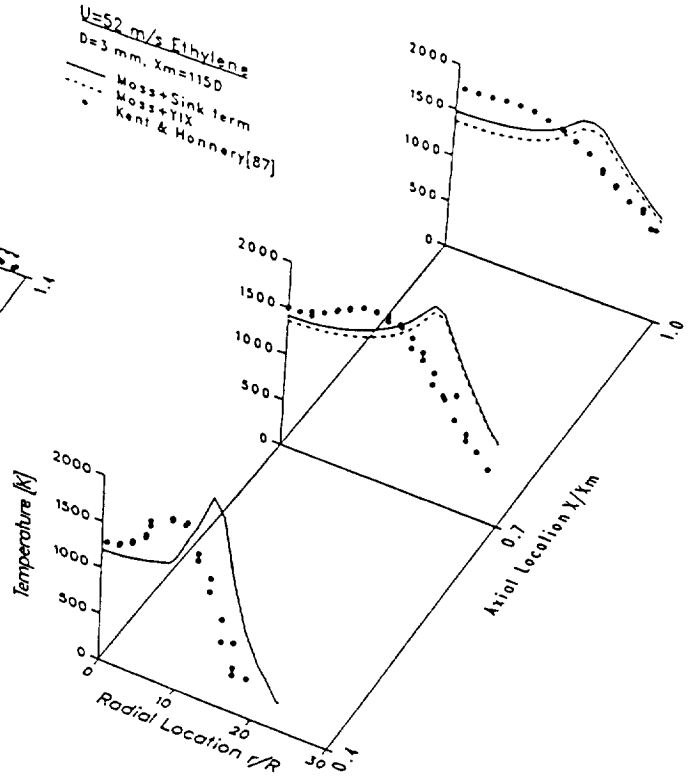

Figure 11. Comparisons of predictions to data for a 1-g 0.61 lpm turbulent ethylene jet diffusion flame.

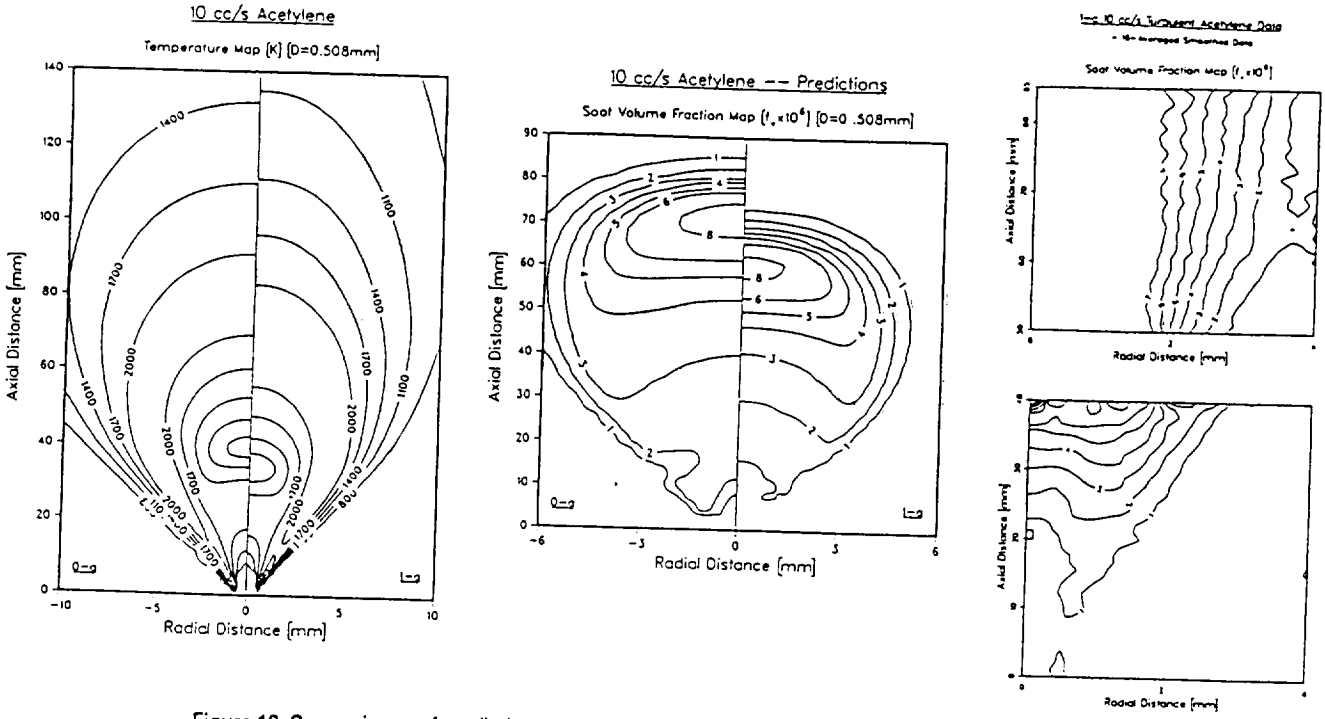

Figure 12. Comparisons of predictions to data for a 1-g 10.0 cc/s turbulent acetylene jet diffusion flame.

ACKNOWLEDGMENTS The authors are indebted to J.-Y. Chen of UC/Berkeley for providing the turbulent flame structure code.

REFERENCES

Bahadori, M. Y., and Edelman, R. B., 1993, "Effects of Buoyancy on Gas Jet Diffusion flames," NASA CR-191109.

Bilger, R. W., 1976, "Turbulent Jet Diffusion Flames," Prog. Energy Comb. Sci., 1, 87-109.

Bilger, R. W., 1977, "Reaction Rates in Diffusion Flames," Comb. Flame, 30, 277-284.

Chen, J.-Y., Kollmann, W., and Dibble, R. W., 1987, "Numerical Computation of Turbulent Free-Shear Flows Using a Block-Tridigonal Solver for a Staggered Grid System," 18th Annual Pittsburgh Conf. Modeling and Simulation.

Edwards, D. K., 1976, "Molecular Gas Band Radiation," Advances in Heat Transfer, Vol. 12, T. F. Irvine, Jr. and J. P. Hamett, Eds., Academic Press, New York, 115-193.

Faeth, G. M., Jeng, S.-M., and Gore, J., 1985, "Radiation from Fires," ASME HTD-Vol. 45 Heat Transfer in Fire and Combustion Systems, 137-151.

Faeth, G. M., and Samuelson, G. S., 1986, "Fast-Reaction Nonpremixed Combustion," Prog. Energy Comb. Sci., 12, 305-372.

Fairweather, M., Jones, W. P., and Lindstedt, R. P., 1992, "Predictions of Radiative Transfer from a Turbulent Reacting Jet in a Cross-Wind," Comb. Flame, 89, 45-63.

Gore, J. P., and Faeth, G. M., 1986, "Structure and Spectral Radiation Properties of Turbulent Ethylene/Air Diffusion Flames," 21st Symp. (Int'l) Comb., 1521-1531.

Gore, J. P., Ip, U.-S., and Sivathanu, Y. R., 1992, "Coupled Structure and Radiation Analysis of Acetylene/Air Flames," J. Heat Transfer, 114, 487-493.

Greenberg, P. S., and Ku, J. C., 1996a, "Soot Volume Fraction Imaging," submitted to Applied Optics.

Greenberg, P. S., and Ku, J. C., 1996b, "Soot Volume Fraction Maps for Normal and Reduced Gravity Laminar Acetylene Jet Diffusion Flames," submitted to Comb. Flame.

Habib, Z. G., and Vervisch, P., 1988, "On the Refractive Index of Soot at Flame Temperature," Comb. Sci. Tech., 59, 261-274.

Hsu, P.-F., and Ku, J. C., 1994, "Radiative Heat Transfer in Finite Cylindrical Enclosures with Nonhomogeneous Participating Media," J Thermophys. and Heat Transfer, 8, 434-440.

Hsu, P.-F., and Ku, J. C., 1995, "Detailed Spectral Radiation Calculations for Nonhomogeneous Soot/Gas Mixtures Based on a Simulated Ethylene Jet Diffusion Flames," ICHMT Int'l Symp. on Radiative Heat Transfer, Kusadasi, Turkey (Aug. 14-18).

Hsu, P.-F., Tan, Z., and Howell, J. R., 1993 "Radiative Transfer by the YIX Method in Nonhomogeneous, Scattering and Non-Gray Medium," J. Thermophys. Heat Transfer, 7, 487-495.

Janicka, J., and Kollmann, W., 1978, "A Two-Variables Formalism for the Treatment of Chemical Reactions in Turbulent H_2-Air Diffusion Flames," 17th Symp. (Int'l) Comb, 421-430.

Jeng, S.-M., and Faeth, G. M., 1984, "Species Concentrations and Turbulent Properties in Buoyant Methane Diffusion Flames," J. Heat Transfer, 106, 721-727.

Kennedy, I. M., Kollmann, W., and Chen, J.-Y., 1990, "A Model for Soot Formation in a Laminar Diffusion Flame," Comb. Flame, 81, 73-85.

Kennedy, I. M., Kollmann, W., and Chen, J.-Y., 1991, "Predictions of Soot in Laminar Diffusion Flames," AIAA Journal, 29, 1452-1457.

Kent, J. H., and Honnery, D., 1987 "Soot and Mixture Fraction in Turbulent Diffusion Flames," Comb. Sci. Tech., 54, 383-397.

Khan, I. M., Greeves, G., and Probert, D. M., 1971, "Air Pollution Control in Transport Engines," Institution of Mechanical Engineers, p. 205.

Khan, I. M., and Greeves, G., 1974, "A Method for Calculating the Formation and Combustion of Soot in Diesel Engines," Chapter 25 in Heat Transfer in Flames, N. H. Afgan and J. M. Beer, Eds., Scripta Book Co.

Ku, J. C., Griffin, D. W., Greenberg, P. S., and Roma, J., 1995a, "Buoyancy-Induced Differences in Soot Morphology," Comb. Flame, 102, 216-218.

Ku, J. C., and Shim, K.-H., 1991, "Optical Diagnostics and Radiative Properties of Simulated Soot Agglomerates," J. Heat Transfer, 113, 953-958.

Ku, J. C., Tong, L., and Greenberg, P. S., 1995b, "Detailed Modeling Analysis for Soot Formation and Radiation in Microgravity Gas Jet Diffusion Flames," NASA Conference Publication 10174, Third International Microgravity Combustion Workshop, 375-380.

Lee, K. B., Thring, M. W., and Beer, J. M., 1962, "On the Rate of Combustion of Soot in a Laminar Sooting Flame," Comb. Flame, 6, 137-145.

Leung, K. M., Lindstedt, R. P., and Jones, W. P., 1991, "A Simplified Reaction Mechanism for Soot Formation in Nonpremixed Flames," Comb. Flame, 87, 289-305.

Lockwood, F. C., and Naguib, A. S., 1975, "The Prediction of the Fluctuations in the Properties of Free, Round-Jet Turbulent Diffusion Flames," Comb. Flame, 24, 109-124.

Menguc, M. P., and Viskanta, R., 1986, "Radiative Transfer in Axisymmetric, Finite Cylindrical Enclosures," J. Heat Transfer, 108, 271-276.

Moss, J. B., Stewart, C. D., and Syed, K. J., 1988, "Flow field Modeling of Soot Formation at Elevated Pressure," 22nd Symp. (Int'l) Comb., 413-423.

Reynolds, W. C., 1986, "The Element Potential Method for Chemical Equilibrium Analysis: Implementation in the Interactive Program STANJAN," Department of Mechanical Engineering, Stanford University.

Rogg, B., 1993 "RUN-1DL: The Cambridge Universal Laminar Flamelet Computer Code," Reduced Kinetic Mechanisms for Applications in Combustion Systems, C. N. Peters and B. Rogg, Eds., Springer-Verlag, Berlin-Heidelberg.

Santoro, R. J., Semerjian, H. C., and Dobbins, R. A., 1983 "Soot Particle Measurements in Diffusion Flames," Comb. Flame, 51, 203-218.

Santoro, R. J., Yeh, T. T., Horvath, J. J., and Semerjian, H. C., 1987, "The Transport and Growth of Soot Particles in Laminar Diffusion Flames," Comb. Sci. Tech., 53, 89-115.

Siegel, R., and Howell, J. R., 1992 Thermal Radiation Heat Transfer, 3rd ed., Hemisphere, Washington, DC.

Sivathanu, Y. R., and Faeth, G. M., 1990a, "Temperature/Soot Volume Faction Correlations in the Fuel Rich Region of Buoyant Turbulent Diffusion Flames," Comb. Flame, 81, 150-165.

Sivathanu, Y. R., and Faeth, G. M., 1990b, "Generalized State Relationships for Scalar Properties in Nonpremixed Hydrocarbon/air Flames," Comb. Flame, 82, 211-230.

Sivathanu, Y. R., Kounalakis, M. E., and Faeth, G. M., 1990, "Soot and Continuum Radiation Statistics of Luminous Turbulent Diffusion Flames," 23rd Symp. (Int'l) Comb., 1543-1550.

Song, T. H., and Viskanta, R., 1987, "Interaction of Radiation with Turbulence: Application to a Combustion System," J. Thermophys. Heat Transfer, Vol. 1, 56-62.

Syed, K. J., Stewart, C. D., and Moss, J. B., 1990, "Modeling Soot Formation and Thermal Radiation in Buoyant Turbulent Diffusion Flames," 23rd Symp. (Int'l) Comb., 1533-1541.

Tan, Z., and Howell, J. R., 1990, "New Numerical Method for Radiation Heat Transfer in Nonhomogeneous Participating Media," J. Thermophys. Heat Transfer, 4, 419-424.

Tong, L, 1995, "A Detailed Modeling of Soot Formation and Radiation in Jet Diffusion Flames under Normal and Reduced Gravity Conditions," Ph. D. Dissertation, Wayne State University.

Tong, T. W., and Skocypec, R. D., 1992, "Summary on Comparison of Radiative Heat Transfer Solutions for a Specified Problem," Developments in Radiative Heat Transfer, S. T. Thynell et al., Eds., ASME HTD-Vol. 203, 235-264.